International Journal of Innovative Technologies
WWW.IJITECH.ORG
ISSN 2321-8665
Volume.06, Issue.01,
January-June, 2018,
Pages:0077-0087

Maximum Power Point Tracking of PV Arrays under PSC for Partial Shadding

PENUMUDI AJAYBABU[1], K. DEEVAN KUMAR[2]
[1]PG Scholar, VRS & YRN College of Engineering and Technology, Chirala, AP, India.
[2]Associate Professor, VRS & YRN College of Engineering and Technology, Chirala, AP, India.

Abstract: One of the most important issues in the operation of a photovoltaic (PV) system is extracting maximum power from the PV array, especially in partial shading condition (PSC). Under PSC, *P–V* characteristic of PV arrays will have multiple peak points, only one of which is global maximum. Conventional maximum power point tracking(MPPT) methods are not able to ex-tract maximum power in this condition. In this paper, a novel two-stage MPPT method is presented to overcome this drawback. In the first stage, a method is proposed to determine the occurrence of PSC, and in the second stage, using a new algorithm that is based on ramp change of the duty cycle and continuous sampling from the *P–V* characteristic of the array, global maximum power point (MPP) of array is reached. Perturb and observe algorithm is then re-activated to trace small changes of the new MPP. Open-loop operation of the proposed method makes its implementation cheap and simple. The method is robust in the face of changing environmental conditions and array characteristics, and has mini-mum negative impact on the connected power system. Simulations in Matlab/Simulink results validate the performance of the proposed methods.

Keywords: Photovoltaic(PV),Partial Shading Condition(PSC), MPPT.

I. INTRODUCTION

In recent years, many places in the world have been experiencing continued shortage of electric power or energy crisis due to their fast increasing demand. To solve this problem, significant efforts of research and development have been given in two areas: Firstly, improve the efficiency of present power conversion and utilization system. Secondly, develop efficient renewable energy generation and conversion systems to supplement conventional fossil fuel based energy supply and eventually replace it. Renewable energy sources offer a promising solution to the energy crisis. The renewable energy generation and conversion system has many advantages over conventional energy supply,e.g.the ability of regeneration, reusability and less pollution. However, the renewable energy generation and conversion technologies are not completely mature yet. There still exist problems such as low efficiency and high cost. The main sources of renewable energy currently under development include solar, wind, hydropower and biomass. These renewable energy sources like solar and wind have shown promise as possible cost efficient alternatives to fossil fuels. Compared to wind energy, the most effective and harmless energy source is probably solar energy. Most renewable sources are based on energy from the sun, geothermal forces and planetary motion in the solar system. Solar, wind, hydropower, wave energy, tidal power, ocean thermal energy conversion, and bio fuels are renewable where as fossil fuels constitute non-renewables. Solar energy is the solar radiation that reaches the earth. Every day Sun radiates or sends out an enormous amount of energy. Broadly, following three approaches are generally followed for utilizing solar energy.

- Absorbing solar energy directly or by using concentrators and then converting into thermal energy for needed applications,
- Converting solar energy into electrical power using photovoltaic or thermoelectric devices, and
- Utilizing solar energy indirectly.

The solar power system has the potential to become one of the main renewable energy sources due to the commercial availability of semiconductor-based photovoltaic devices, reduction in the system cost and development of power electronic technologies. In recent years, the solar power generation and conversion technology is developing rapidly. One of the important tasks is to make solar power generation and conversion system more efficient and more reliable. Photovoltaic system converts solar energy into electrical energy using solar cells. The major drawbacks of solar PV systems are their high initial cost and the low efficiency. Also, the performance of the solar cell depends on the variation in solar radiation and ambient temperature. Currently, solar panels are not very efficient with only about 12 ~ 20% efficiency in their ability to convert sunlight to electrical power. The efficiency can drop further due to other factors such as solar panel temperature and load conditions. In order to maximize the power derived from the solar panel, it is important to operate the panel at its optimal power point. To achieve this, a type of charge controller called a Maximum Power Point Tracker is designed and implemented. The proposed Maximum Power Point Tracker must be able to accurately track the constantly varying operating point where the maximum power is delivered in order to increase the efficiency of the solar cell.

Here has been increasing interest in photovoltaic (PV) **T**systems as a renewable energy source in recent years. PV systems can be operated as grid-connected or stand-alone struc-tures. The main element of a PV system is PV array that

is a set of PV modules connected in series and parallel. In a PV array, voltage and current have a nonlinear relation, and only in one operating voltage, maximum power is generated. Therefore, extracting maximum power from a PV system in all operation conditions is the main target of its control. To date, numer-ous maximum power point tracking (MPPT) techniques have been presented and implemented. Some of the conventional and most popular ones are perturb and observe (P&O), incremen-tal conductance (IC), and short-circuit current, and open-circuit voltage. Some techniques are also presented based on artificial intelligence, such as fuzzy logic and neural network, but have more computation load [1]. A condition in which the entire modules of an array do not receive the same solar irradiance is called partial shading condition (PSC). PSCs are inevitable especially in solar systems installed in urban areas and in areas where low moving clouds are common [2]. If the control system cannot detect and react to this situation, the PV system will be diverted from the optimal operation mode. In PSC, because of bypass diodes in parallel with each module, *P–V* characteristic of the array has multi-ple peak points [3]. Conventional MPPT techniques are unable to identify the global maximum power point (GMPP) in PSC, and usually track local peaks. Therefore, developing new MPPT techniques for dealing with PSC is necessary.

In recent years, many techniques have been presented for MPPT under PSC [4]–[21]. Most of these techniques consist of two steps to attain GMPP. In the first step, the neighborhood of GMPP is determined, and in the second step that usually uses conventional MPPT methods such as P&O, the exact GMPP is obtained. In [4], after PSC detection, by moving on the load line that is based on short-circuit current and open-circuit voltage of the array, the operating point moves to the vicinity of the GMPP, and in the second step, the operating point converges to it. One can easily show that this technique is unable to track the GMPP in all PSCs [5]. The proposed method in [6] is basically a P&O algorithm that its voltage step sizes are determined based on dividing rectangles method. This technique does not guarantee reaching the GMPP. A neural network training for different PSCs is presented in [7], which is system dependent and needs measurement of solar irradiance level and temperature. Abdalla *et al*. [8] uses a multilevel converter and a new control algorithm to overcome the PSC problem. A novel distributed maximum power point tracking is proposed in [9] wherein the current of each module is compensated by regulating its voltage at the respective maximum power point (MPP) value by connecting a fly-back dc–dc converter in parallel with each module. The proposed MPPT in [10] uses a controllable current transformer (CCT) disposed at the terminal of each PV module, permitting compatible current in the series path of a PV string.

The CCT output current can be regulated using a dependent current source according to the MPPT algorithm. Although accuracy of these methods is high and they decrease the effect of PS on the array power, their implementation is expensive. In [1], when the PV power suddenly changes beyond a certain threshold, the proposed method starts sampling the *P–V* characteristic of the array in 60% − 70% of V_{oc-mod} (open-circuit voltage of module) intervals, and at each sample, in case of sign change of *dP/dV* , P&O technique is utilized to determine the local peak. Finally, by comparing all peaks, the GMPP is determined. The proposed method in [2] is also based on the method suggested in [1] and is similar to [3]. Dependency on V_{oc-mod} , a parameter that changes with environmental conditions, and low speed of the algorithm due to high sampling number are the weak points of these algorithms.The method proposed in[4] has good performance, but it is required to measure the voltage of each module. The method proposed in[5] is based on IC and sampling the *P–V* characteristic of the array in distances of0.8 V_{oc-mod} . It limits the search area for GMPP as in [1], and yields suitable results, but needs high sampling number. Wang *et al*. [2] proposes two methods: the first approach samples the *P–V* curve and limits the search area based on short-circuit current of the modules and the highest local power. As it is mentioned in [2], this method has high accuracy with low speed.

Therefore, a second approach is pro-posed that estimates the local MPP power by measuring the currents of bypass diodes of the modules. Although the speed of tracking is improved, its implementation cost is high. Studying MPPT as an optimization problem resulted in us-ing evolutionary optimization methods such as particle swarm, simulated annealing, and colony of flashing fireflies to find the GMPP [16]–[21]. In these methods, GMPP is obtained by sampling different points of the array *P–V* characteristic. These methods are mostly successful, but their sampling num-ber is high. Since the GMPP can occur in a wide range of the *P–V* characteristic, initial sampling must cover the entire curve. Boost converters experience some transients to settle the volt-age of the PV array [22], [23]. Then, as the sampling number increases, the speed of MPPT decreases. In [16]–[19], a typi-cal version of Particle Swarm Optimization (PSO) algorithm is used that has low speed. In [18], the PSO method is modified to improve its speed and complexity. A method based on firefly algorithm is proposed in [20] that has better speed and efficiency in comparison to PSO-based algorithms. The proposed method in [21] uses the simulated annealing algorithm for MPPT under PSC. It is clear from the presented results that the samplings number is high and speed of GMPPT is even lower than the PSO-based method, while its accuracy is higher.

Generally, a good MPPT algorithm that is also successful in the PSC should have the following properties:

- tracking the MPP rapidly for getting high efficiency;
- simple implementation with a low computational load;
- requiring less and cheaper sensors (removing current sensors of boost converter reduces the cost dramatically).

Imposing minimum disturbance to the connected grid. Another issue that is less addressed in the literature is detection of the PS occurrence. Before applying any MPPT process under PSC, it is necessary to detect its incidence.

Until now, no special algorithm is presented to deal with this issue, and a sudden big change in the array power is commonly used as PS occurrence indicator [1], [2]. Determination of a threshold for big power change to distinguish between PSC and uniform irradiance condition(UIC) perfectly is not straight forward. Also, it is possible that in some situations, especially changing the PS pattern, no big power change is observed. Another presented method is based on the fact that in PSC, there is big difference between the array currents in the low and high voltages of the array [8]. This method needs to sample from the array current in low and high voltages, and therefore, imposes a big disturbance on the PV power and the connected grid.

II. PROPOSED METHOD

In this project, the following symbol definitions are used. $V_{\text{o-cmod}}$ is open-circuit voltage of PV module, $V_{\text{oc–str}}$ is open-circuit voltage of PV string, $V_{\text{o c–arr}}$ is open-circuit voltage of PV array, $V_{\text{m pp}}$ is the voltage of MPP, $V_{\text{m pp–m o d}}$ is the volt-age of module at its MPP, $V_{\text{m pp–str}}$ is the voltage of string at its MPP at UIC, and $V_{\text{m pp–arr}}$ is array voltage at MPP under UIC. The module current is maximum at $V = 0$ and is known as short-circuit current (I_{sc}). For voltages above $V_{\text{o c–m o d}}$, there will be negative current, but a blocking diode will force it to zero. In Fig. 2(a), *I–V* and *P–V* characteristics of a typical solar mod-ule under UIC are presented. In UIC, the MPP of module and array are unique and are achieved at $V_{\text{m pp–m o d}} = \alpha V_{\text{o c–m o d}}$ and $V_{\text{m pp–arr}} = \alpha V_{\text{o c–arr}} = N_{\text{s}}\ V_{\text{m pp–m o d}}$, respectively; α is a coefficient that is dependent on model parameters of solar module.

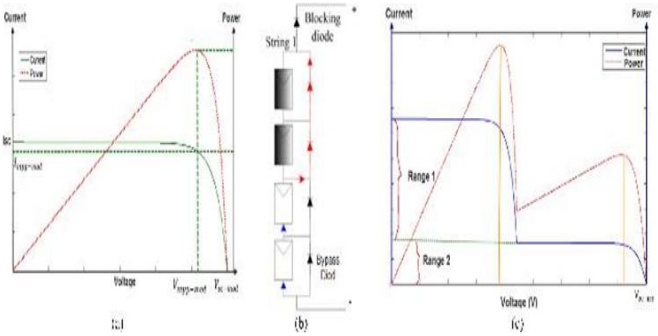

Fig2. (a) *P–V* and *I–V* characteristics of a typical PV module. (b) Structure of a sample shaded string. (c) *P–V* and *I–V* characteristics of the shaded string.

B. Partially Shaded Condition

For simplicity, it is initially supposed that the array under PSC is subjected to two different irradiance levels. Modules that receive high irradiance level (*HS*) are called insolated modules and those which receive lower irradiance level (*LS*) are named shaded modules. The insolated modules of a string drive the string current. Therefore, portion of the string current that is greater than the generated current of shaded modules passes through parallel resistance of the shaded modules and generates negative voltage across them. Thus, the shaded modules consume power instead of generating it. In this condition, not only the overall efficiency drops, but also the shaded modules may be damaged due to hot spots. To prevent this condition, a bypass diode is connected in parallel to each module, to let the extra current of the string pass through it. Consequently, the voltage across that module will be about −0.7V and efficiency of the string will improve. The structure of a sample shaded array is shown in Fig2(b). Further details about the modeling of array in PSC are given in[3]–[24].

C. Critical Observations Under Partially Shading Condition

Fig. 2(b) and (c) show the structure and *I–V* and *P–V* char-acteristics of a typical partially shaded string with $N_{\text{s}} = 4$ series modules, $n_{\text{sh}} = 2$ shaded modules, and $n_{\text{in}} = 2$ inso-lated modules. As explained in the previous section, for cur-rents higher than I_{sc} of shaded modules (Range 1), their by-pass diodes conduct extra current and cause the voltage across them to be about −0.7 to −1 V. In this situation, the string voltage is equally divided only between the insolated modules. For currents lower than I_{sc} of the shaded modules (Range 2), insolated modules operate in approximately constant voltage area, and therefore, the voltage across each of these modules will be more than $V_{\text{m pp–m o d}}$ and close to $V_{\text{o c–m o d}}$. The *P–V* characteristic of the string has two MPPs. The first one is at $V_{\text{m pp–1}} \approx n_{\text{in}}\ V_{\text{m pp–m o d}} - n_{\text{sh}} * 0.7$ and the second MPP oc-curs when the voltage of one shaded module is about $V_{\text{m pp –m o d}}$. The string voltage in this local MPP ($V_{\text{m pp–2}}$) is bound as fol-lows:

$$^{N}s^{V}\text{mpp}-\text{mod}^{<V}\text{mpp}-2^{<n}\text{sh}^{V}\text{mpp}-\text{mod}^{+n}\text{in}^{V}\text{ocmod} \qquad (3)$$

When the irradiance ratio *IR = HS/LS* decreases, $V_{\text{m pp–2}}$ gets close to the lower bound of (3), and as it increases, $V_{\text{m pp–2}}$ moves toward the upper limit. Also, when $K = n_{\text{sh}} / n_{\text{in}}$ is too high, the upper limit of (3) approaches the lower limit, and $V_{\text{m pp–2}}$ gets close to it. According to the above discussion, it can be shown that in one string, the minimum difference between the voltages of two local MPPs is more than $V_{\text{m pp–m o d}}$.

III. OPEN-LOOP CONTROL OF BOOST CONVERTER IN THE PV SYSTEM

In Fig3, a two-stage grid connected solar system is shown. In the first stage, dc/dc boost converter plays the main role in absorbing power from the PV array by controlling its voltage. In the second stage, an inverter controls the output voltage of the dc/dc converter and generates ac voltage to connect the solar system to the grid. Because of the dc link capacitor between the boost converter and the inverter, there is little coupling between the two stages and the stages can be studied separately [5]. Generally, there are two control approaches for regulation of a PV array using boost converter; i.e., close-loop and open-loop controls. Weidong *et al*. [3] shows that in a PV array connected to the boost converter, the worst case from stability and dynamic response points of view, occurs when the array operates in constant current region and low irradiance level, where dynamic resistance of the array has its largest negative value. Due to dependency of the system dynamic response to the operating point and environmental conditions, it is not pos-sible to control the array voltage in

close-loop fashion using a single-loop PI voltage controller properly, and another inner control loop is required (boost converter inductor current loop) to reach desired dynamic response of the system (high-speed, low-transient, and zero steady-state error) [3]. This two-loop control method needs two PI controllers and an expensive cur-rent sensor. In contrast, in open-loop control, which is a common method for boost converters control, there is no feedback, and the appropriate input voltage is generated considering the rela-tion between the input voltage (v_{in}) and output voltage (v_o) of the converter as in (4)

$$v_{in} = v_{pv} = (1 - D)v_o \quad (4)$$

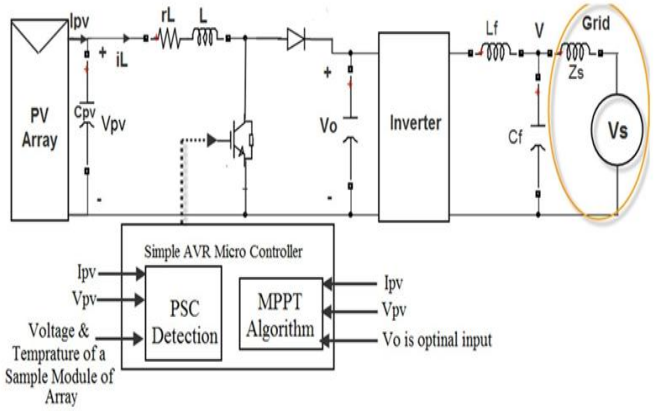

Fig3. Overview of a two-stage grid connected PV system structure.

In this method, it is not necessary to measure the boost con-verter inductor current and an expensive current sensor is saved. However, the system response may have some steady-state er-ror and more transients than the close-loop method. One of the important parameters in MPPT of a PV system is the sampling time. After applying a new command voltage (v_{in}^{ref}) to the con-verter, to prevent instability and disruption in MPPT, sampling from the array voltage and current must be done after settling the system transient response. Therefore, sampling time period must be more than this settling time. For further analysis, response of a PV array connected to a boost converter with open-loop control is studied through simulation in Matlab/Simulink environment. Converter parameters are presented in Table I and the simulated PV array has $V_{o\ c-arr}$ = 130 V and I_{sc} = 8 A. Output voltage of the boost converter is also considered constant at 250V. Both the switching and averaged state-space models of the system are simulated and their responses to step and ramp com-mand signals by open-loop control are shown in Fig. 4. Following conclusions are made from the system response:

- Responses of the accurate switching model and the aver-aged state-space model are almost identical.
- The system response to step and ramp command signals contain some steady-state error. This error can deterio-rate the MPPT methods that are based on sampling from specific points of the array's *P–V* characteristic [13].
- Oscillation, overshoot, and settling time of the system to step commands is high, especially when the operating point in the constant current region of the PV array, which impose higher switching stress and losses. In contrast, the ramp response has negligible transient.
- Settling time of the system step response is about 15 ms.

Thus, for MPPT application, sampling time must be more than 15 ms. It is noteworthy that r_L is considered high, while in practice, for better efficiency, it is lower and results in higher settling time.

IV. PSC DETECTION

In this section, an algorithm for PSC detection is presented which is based on three criteria. Also, performance of the final algorithm is evaluated in various PS patterns.

A. PSI Index as PSC Detection Criterion

The first proposed criterion is based on a new index that is defined as follows, The criterion is normalized derivative of the PV array power respect to the array voltage at $V_{m\ pp-arr} = N_s\ V_{m\ pp-mod} = V_{m\ pp-str}$, which is similar to that used in IC method for MPPT. At UIC, PSI is zero. Under PSC, however, the local MPP volt-age changes from $V_{m\ pp-arr}$, and therefore, PSI is not zero and is dependent on the shading pattern.

$$PSI = \frac{\Delta P}{\Delta V.P}|_{V_{mpp-arr}} = \frac{\frac{\partial P}{\partial V}}{V.I}|_{V_{mpp-arr}} = \frac{\frac{\partial (VI)}{\partial V}}{V.I}|_{V_{mpp-arr}} = \frac{1}{V_{mpp-arr}} + \frac{\partial I}{I.\partial V}|_{V_{mpp-arr}}. \quad (5)$$

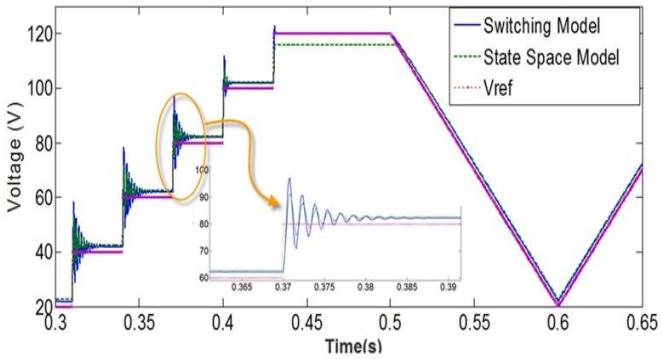

Fig4. Response of switching and averaged state space models of boost converter in PV system to step and ramp commands.

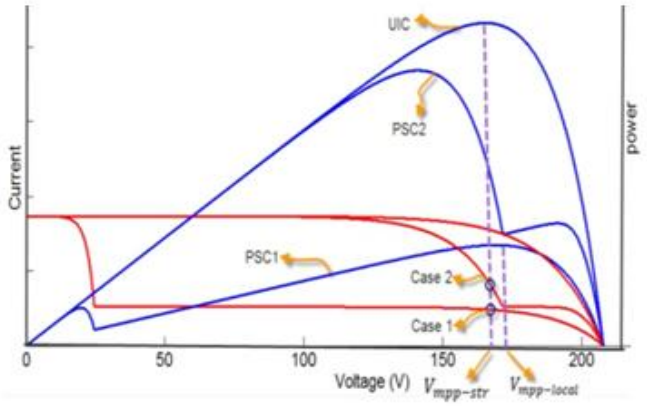

Fig5. *I–V* and *P–V* characteristics of PV string in different PSCs.

According to Section II, when a PV string is under PSC, the voltage across the shaded module ($V_{mod-shaded}$) at $V_{mpp-str} = N_s V_{mpp-mod}$ is bound as follows:

$$\frac{N_s V_{mpp-mod} - n_{in} V_{oc-mod}}{N_s - n_{in}} < V_{mod-shaded} < V_{mpp-mod}. \quad (6)$$

From (6), two cases may arise for $I \frac{\partial I}{\partial V}|_{V mpp-arr}$:

1. $N_s V_{mpp-mod} > n_{in} V_{oc-mod}$ (see Fig. 5. Case1): In this condition, $V_{mod-shaded}$ is positive and the absolute value of is less than its value in UIC, the local MPP of the string is in$V > V_{mpp-arr}$, and PSI is positive.
2. $N_s V_{mpp-mod} < n_{in} V_{oc-mod}$ (see Fig. 5. Case2):

In this case, the shaded modules are bypassed with the by-pass diodes, and $V_{mod-shaded} \approx -0.7V$. The insolated modules operate in the constant voltage region. Therefore, is much bigger than its value in UIC; PSI is negative and local MPP of the string is $^{in}V < V_{mpp-arr}$. To investigate the effectiveness of the PSI index in PSC detec-tion, behavior of a sample string, as a representative of an array, is analyzed in different PS patterns. For simplicity and without loss of generally, only two irradiance levels are considered in PSs.

$$\begin{aligned} P_{mpp-2} &= V_{mpp-2} I_{mpp-2} \approx V_{mpp-2} \cdot \left(\frac{1}{IR}\right) . I_{mpp-1} \\ &> (K+1)\, n_{in} V_{mpp-mod} \cdot \left(\frac{1}{IR}\right) . I_{mpp-1} \\ &= (K+1) \left(\frac{1}{IR}\right) P_{mpp-1}. \end{aligned} \quad (7)$$

It is obvious that when *IR* is too low or *K* is too high (the same situation that PSI index may be near zero, e.g., PSC1 in Fig5), P_{mpp-2} will be much greater than P_{mpp-1}. Therefore, if the PSI index mistakes in detection of this PSC, the conventional P&O algorithm used in the UICs tracks the second MPP which is the GMPPT.

B. Updating $V_{mpp-arr}$ and Final PS Detection Criteria

Until now, it was supposed that $V_{mpp-arr}$ is available for PSI evaluation. In practice, $V_{mpp-arr}$ and $V_{mpp-mod}$ are dependent on the type of modules and temperature as in (8); and also, there is some difference between the temperatures of the shaded and insolated modules

$$\begin{aligned} V_{mpp-arr} &= V_{mpp-arr-SC} * (1 - \rho_{arr} . (T - 25)) \\ &= \sum_{i=1}^{N_s} V_{mpp-mod-SC} * (1 - \rho_{mod-i} . (T_i - 25)) \end{aligned} \quad (8)$$

where *V*mpp−arr−SC and *V*mpp−mod−SC are *V*mpp−arr and *V*mpp−mod in standard condition (S = 1 kW/m2 ,T = 25C.), respectively. T is temperature and ρarr and ρmod are the temperature dependency coefficients of *V*mpp−arr and *V*mpp−mod, respectively. In the UIC, the operating voltage of the array is*V*mmp−arr . Therefore, *V*mmp−arr is available continuously.

Also, its slight dependence on irradiance level can be updated easily, using the array current at *V*mmp−arr . Under PSC, the operating voltage is not*V*mmp−arr . Consequently, *V*mmp−arr that is dominantly dependent on the temperature of the array is not available. If the PS is due to relatively fast transient phenomena like the passing clouds, the temperature cannot change rapidly, and therefore, it is almost identical in all modules. Otherwise, temperatures of the shaded and insolated modules are different; and this temperature difference is proportional to the difference of the radiation levels. Hence, for updating*V*mmp−arr , temperatures of all modules must be measured, a requirement that is not economical. Hence, in the proposed algorithm only the temperature of one sample module is used for updating*V*mmp−arr according to (8) (*V*mmp−arr and *V*mmp−mod are updated using ρarr and ρmod, respectively). In this situation, it is not clear whether the sample module is insolated or shaded. Accordingly, three cases may be fronted as follows.

- The whole array is in UIC, and therefore, the temperature of all modules is the same as the sample module temperature. Thus, there is no error in updating Vmpp−arr in this case, and UIC can be detected using the PSI index.
- The array is in PSC and the sample module is insolated. In this case because of the negative value of ρmod for all types of modules and ρarr in (8), the updated value of Vmpp−arr will be less than its real value. Therefore, the calculated value of PSI and the difference between the real local MPP voltage and the updated Vmpp−arr (named |ΔVmpp−arr |) will be greater than its real value. Hence, PS detection becomes easier.
- The array is in PSC and the sample module is shaded. In this case, also because of the negative value of ρarr , the updated value of *V*mpp−arr is greater than its real value. Therefore, the calculated value of PSI and the difference between the local MPP voltage and the updated *V*mpp−arr will be smaller than its real value and may be even zero.

Therefore, success of the proposed algorithm may be affected. In this situation, voltage of the sample module is measured while the array voltage is at updated value of*V*mpp−arr . Clearly, voltage of the sample module at this point is quite different from the updated value of*V*mpp−mod (named |Δ*V*mpp−mod|) when the array is under PSC. Otherwise, their difference will be nearly zero. This modification ensures success of the proposed algorithm for PS detection. According to the above discussion, the PSI index criterion is reinforced with two other criteria. These two criteria are defined based on normalized values of |Δ*V*mpp−arr| and |Δ*V*mpp−mod| that are defined in the above. Finally, the criteria for PS detection will be follows

$$\begin{aligned} &|\mathrm{PSI}| > 0.001 \\ &\left|\frac{\Delta V_{mpp-arr}}{V_{mpp-arr}}\right| > 0.02 \\ &\left|\frac{\Delta V_{mpp-mod}}{V_{mpp-mod}}\right| > 0.02. \end{aligned} \quad (9)$$

The specified thresholds in (9) are determined according to the simulations of many PS scenarios on various structures of PV array. Based on these criteria, the array is in the PSC if

at least one of these conditions is met. In Fig. 6, a flow chart of the proposed algorithm for PS detection is shown. The proposed PSC detection does not impose any considerable disturbance on the system, since PSI is evaluated at *V*mpp−arr . It is noteworthy that *ρ*arr and *ρ*mod may be nonidentical because the module models in the array may differ. Also, *ρ*arr , *ρ*mod, *V*mpp−arr−sc , and *V*mpp−mod−sc may change due to aging. Nevertheless, they can easily be updated online when the array is under UIC. For the sake of brevity, their updating process is not explained here. However, it can easily be shown that the effectiveness of the algorithm is independent from uniformity of modules and their aging. So far, the proposed algorithm is studied in a string of series modules. In (10), it is shown that PSI of an array is the weighted average PSI of individual strings, and therefore, using the PSI and two other criteria in (9) suffices for PS detection in any array

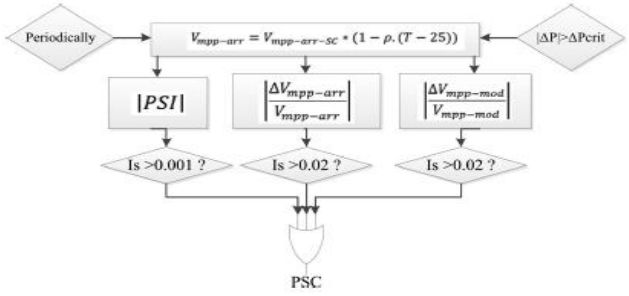

Fig. 6. Flow chart of the proposed algorithms for PS detection.

$$\mathrm{PSI} = \frac{\Delta P}{\Delta V.P}\Big|_{V_{\mathrm{mpp-array}}} = \frac{\sum^{\Delta} P_i}{\Delta V.\sum_i^P}\Big|_{V_{\mathrm{mpp-array}}} = \sum_i^{\mathrm{PSI}} \frac{P_i}{\sum_i^P} \qquad (10)$$

where *Pi* and Δ*Pi* are the power of string *i* and its differentiate, respectively.

In this simulation, the modules are under three different irradiations with the following associated temperatures: (S_1 = 0.9 kw/m^3 , T_1= 35C),(S_2=0.6 kw/m^3 , T_2=30C), and (S_3= 0.3kw/m^3 , T_3=25C). Series and shunt resistances of the modules are also considered in the simulations.

TABLE II
ELECTRICAL DATA OF MODULE ND195R1S IN STANDARD TEST CONDITION

P_{max}	V_{oc}	I_{sc}	I_{mpp}	V_{mpp}	P_{max} Termal Coefficeint	ρ_{mod}
195	29.7	8.68	23.6	8.27	−0.44%/C	−0.329%/C

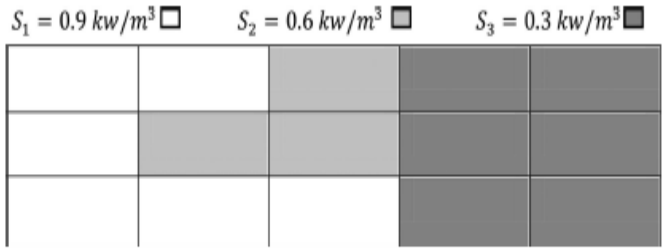

Fig. 7. Simulated array configuration (indicates the sample module).

Results of five different PSC simulations are presented in Ta-ble III. Patterns of the PSCs on the array are presented with a ternary digit for each string of the array. These digits are the number of the modules in each string with (S_1 , T_1), (S_2 , T_2), and (S_3 , T_3), respectively. In these simulations, it is assumed that the temperature and voltage of the marked module in Fig. 7 is measured. As it is clear from Table III, the PSI index fails only in the detection of PSC5, and the third criterion fails only in the detection of PSC2. But using all criteria in (9) makes the algorithm successful in all cases. The proposed method has complete success in detection of all simulated PS patterns. Con-sidering the three criteria in (9) has resulted in good robustness of the method. As it was mentioned previously, robustness of the proposed method is reduced only under the PSCs that *K* is too high and *IR* is too low, and it may be possible that the proposed method does not detect the PSC. In these situations, as proved in part B of this section, the local MPP, which is near $V_{m\ pp-arr}$, is the GMPP and the conventional P&O algorithm tracks it. Therefore, the final goal that is GMPPT is not missed.

TABLE III
RESULTS OF PSC DETECTION IN SAMPLE PSCS

	PSC1	PSC2	PSC3	PSC4	PSC5
PS Patterns	2-2-1	5-0-0	0-1-4	1-1-3	1-1-3
	1-3-1	3-1-1	0-0-5	1-1-3	5-0-0
	3-2-0	3-2-0	1-1-3	1-0-4	4-0-1
|PSI|	0.008	0.0036	0.002	0.003	4.00E-04
$\left\|\frac{\Delta V_{mpp-arr}}{V_{mpp-arr}}\right\|$	0.09	0.04	0.022	0.03	0.003
$\left\|\frac{\Delta V_{mpp-mod}}{V_{mpp-mod}}\right\|$	0.3	0	0.03	0.08	−0.08
PSC	yes	yes	yes	yes	yes

It is worth comparing the proposed PSC detection method with that of[1][2]. Their method is based on observing a big power change, and is sensitive to the relevant threshold: a smaller threshold may cause a wrong detection of PSC, and a bigger one may result in missing it. In contrast, the proposed method in this paper is activated in two ways: 1) periodically, 2) after observing a noticeable power change. For perfect detection of PS, the threshold of this power change can be set to lower values, because after observing the change, the criteria in (9) will be examined to rule out wrong PSC candidates. Also, in comparison to the method used in [8], which samples the array current in low and up voltages to detect PSC, the proposed method in this paper does not impose any big disturbance on the system as the method of [8] does.

V. PROPOSED ALGORITHM FOR MPPT UNDER PSC

Heuristic algorithm based methods such as PSO, as well as most of other methods forMPPT in PSC, need to sample the *P–V* characteristic of the array in different voltages of the search area. Noting to the settling time of boost converter to step commands, these methods have low speed in GMPPT. MPPT is a time varying optimization problem, in which the objective function evaluation is done physically; i.e., by applying specific voltages to the array, its output power is measured after settling its voltage, whereas in the numerical

optimization problems, function evaluation is done numerically and imposes calculation burden on the processor. As mentioned in Section III, sampling time period for MPPT must be greater than the settling time of the boost converter. This settling time depends on the design and operating point of PV array. Maximum settling time of the boost converter used in experiment and simulations of this paper is about 20 ms. According to Section II, under PSC, the GMPP is in the following voltage region that must be searched for GMPPT:

$$V\text{mpp}-\text{mod} < V < V\text{oc}-\text{arr}\,. \qquad (11)$$

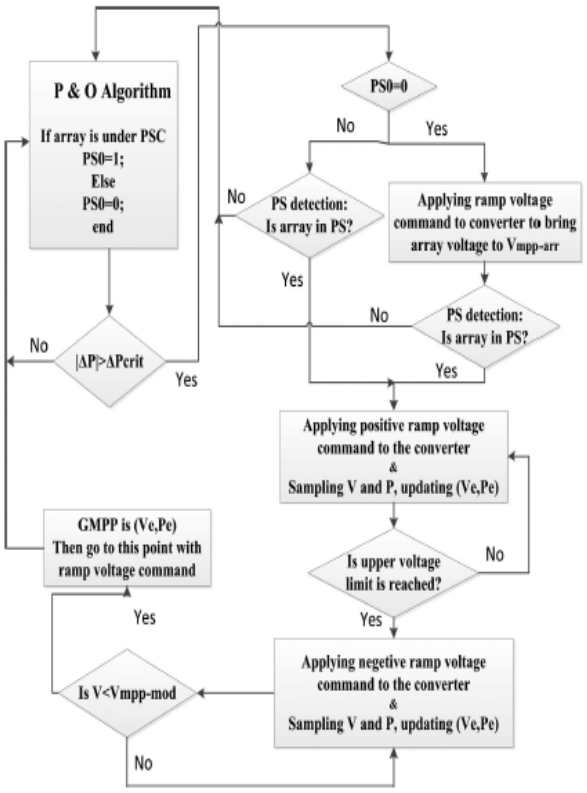

Fig. 8. Flow chart of the proposed algorithms for MPP tracking under PSC.

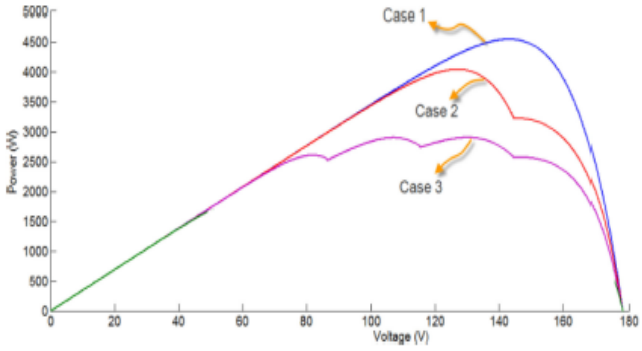

Fig. 9. *P–V* characteristics of array in UIC and two different PSCs.

A straight solution for GMPPT with minimum steps is that sampling from *P–V* characteristic of the array be done only in specific points[3]. In practice, these methods rely on approximations and cannot guarantee the GMPPT. When sampling from the array power is done in *V*1 and *V*2 , respectively; indeed the array voltage experiences all voltages between *V*1 and *V*2 continuously. This is due to the fact that the voltage of the parallel capacitor with the array cannot change steeply. Therefore, almost in all of the MPPT methods, the array experiences all voltages of (11). According to the above discussion, two important facts inspire using ramp voltage as the command signal of converter to search the voltage region of (11) for GMPPT:

- In contrast to the response of the boost converter to step commands, settling time and transient of the boost converter to ramp command is nearly zero (see Fig. 4).
- PV arrays do not have considerable dynamics and can be assumed static. Unlike dynamic systems, then, the measured power at each moment is related to the array voltage at the same moment, corresponding to a point on the *P–V* characteristic of the array.

Thus, the concept of scanning *I–V* characteristic of the array with adjustable high speed ramp command voltage (or ramp change of duty cycle) is proposed in this paper. Along with this ramp input, the array voltage and current is sampled continuously with proper rate. In two different situations that may occur for the PV array, the proposed algorithm for GMPPT operates as follows: 1) While the array is under UIC and operates at ($V1 = V\text{mpp}-\text{arr}$, $P1$), a PS occurs and the operating point changes to ($V2 = V1$, $P2$). The proposed PSC detection algorithm is initiated by this power change, and determines whether the array is still at UIC or has undergone PSC. If no PS is detected, P&O algorithm is called. Otherwise, the proposed MPPT algorithm is activated. Based on the proposed MPPT method, the maximum array power during MPPT process and its corresponding voltage (Ve, Pe) are initialized with ($V2$, $P2$). Then, a positive ramp voltage command, starting from $V1$, is applied to the boost converter according to (4). For this purpose, the duty cycle can also be changed with ramp function, without need to knowthe output voltage (vo) of the boost converter.Consequently, the array voltage changes ramp-likely as shown in Fig10(a).

Simultaneously, the array voltage$V$ (t), which may have some error from the command voltage, and its power $P(t)$ are sampled as ($Vs = V(t)$, $Ps = P(t)$). At each moment, if Ps is greater thanPe , then (Ve, Pe) is updated with ($Ve = Vs$, $Pe = Ps$). This process continues until the array voltage reaches to $V\text{oc}-\text{arr}$. Then, the command voltage ramp sign is inverted and the array voltage is reduced ramp-likely. Updating (Ve, Pe) is continued until the voltage reaches to$V\text{mpp}-\text{mod}$. Finally, GMPP of the array will be the final value of the(Ve, Pe). Then, the array voltage is drived to Ve and the P&O algorithm is called to resume the local MPPT around this operating point.2) The array is under PSC and shading pattern changes. In this case, based on the proposed concept, ramp voltage command is applied to the converter to bring the array voltage to$V\text{mpp}-\text{arr}$ .At this point, PS detection criteria are checked to determine if the array is at UIC or under PSC. If no PS is detected, P&O algorithm is called. Otherwise, MPPTprocess is started by applying positive ramp voltage command to the converter. The rest of the process is same as

explained in Fig. 10(a). To limit the search region for GMPPT, further analyses are presented as follows, Assume a sample operating point of the array as (*Vs*, *Is*). It is known that when the array voltage increases, its current decreases. Therefore, the array current (*I*arr) for*V* >*Vs* is lower than *Is* . Hence

$$P\text{arr}(V > Vs) = V\,I\text{arr} < VIs . \quad (12)$$

In addition, because the maximum voltage of the array is

$$V\text{oc}-\text{arr}\ P\text{arr}(V > Vs) < V\text{oc}-\text{arr}Is . \quad (13)$$

Based on the above arguments, during positive ramp command, at any point in which *V*oc−arr*Is* is less than the last updated value for MPP (*Pe*), the array power will also be less than *Pe* at all upper voltages. Therefore, continuing the positive ramp command is not required. In other words, the search region will be limited to *Vs* in which,

$$V\text{oc}-\text{arr}Is < Pe \quad (14)$$

Whenever PS occurs after a UIC, negative ramp of MPPT process is bound as follows. For the voltages that VIsc < Pe the array power is less than Pe and it is not needed to search this region. Hence, lower voltage of search region will be Vs that

$$\text{Vs} < Pe/I\text{sc} \quad (15)$$

Besides, MPP current of PV arrays under UIC is about 0.9*I*sc [3], and therefore, *I*sc is approximately known in term of *I*mpp−arr . One notes that the proposed MPPT method guarantees convergence to the GMPP under any PSC. The reason is that the voltage region (11) is considered completely, and sampling from the voltage and power of the array is done in the entire region, not at some special points. Furthermore, the proposed MPPT method does not need any electrical characteristics of the PV array except to *V*oc−arr which is used to define the search region. All MPPT methods need to know *V*oc−arr to know the search region. Besides, the exact value of *V*oc−arr is not necessary, and its approximate value can be determined in term of *V*mpp−arr . Flow chart of the proposed algorithm for MPPT in PSC is shown in Fig. 8. The ramp voltage can be implemented either with an analog rate limiter or digitally with small step changes in duty cycle. For selection of the ramp rate, the following points are noted. Sampling rate of the array voltage and current must be coordinated with the ramp rate of command voltage. For example, suppose a PV array with *V*oc−arr = 200 V. To reach the GMPP voltage at about 50 ms, the voltage ramp is selected *R* = 200/0.05 = 4000 V/s. PV arrays have very fast dynamics because of their current leakage to ground, which are negligible and ignored in MPPT process. Theoretically, using very excessive ramp rates in the range of those fast dynamics, may deteriorate performance of the proposed method.

However, this is impractical, and as mentioned earlier, the PV arrays are dealt as static systems. When a ramp command voltage is applied to the boost converter, its voltage changes in proportion to the ramp rate of command voltage, but it may have some steadystate error and very little transients (see Figs. 4, 10, 11). However, in the proposed algorithm, sampling from the array voltage and current is done continuously, and it is not necessary that the array voltage be the same as the command voltage. Therefore, imperfect response of the boost converter does not imply any limitation on the proposed method. The last concern is that excessive increasing of the ramp rate results in high *dP*pv/*dt* during GMPPT, which can disturb the connected grid. Nevertheless, as it is shown in the next section, selecting the voltage ramp as 4000 V/s results in fast MPP tracking and sufficiently low disturbance.

VI. SIMULINK MODELS AND RESULTS

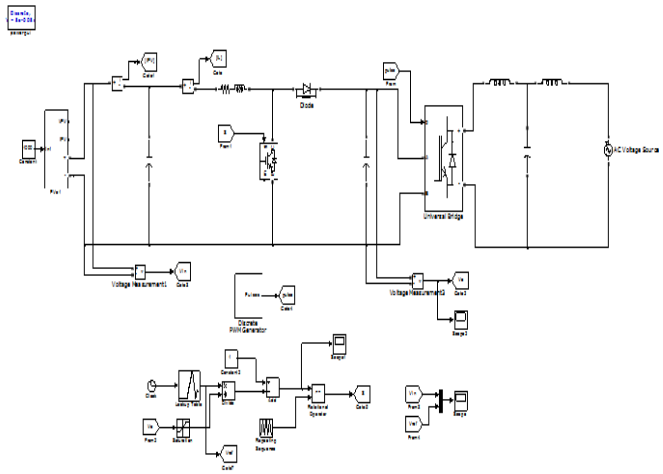

Fig10. Complete Simulink model with conventional method.

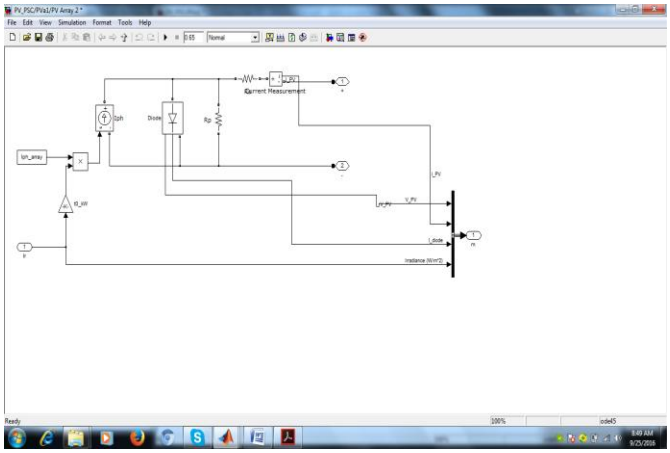

Fig12. Simulink model for v array.

Fig13. Reference signal for dc converter gating signal generation.

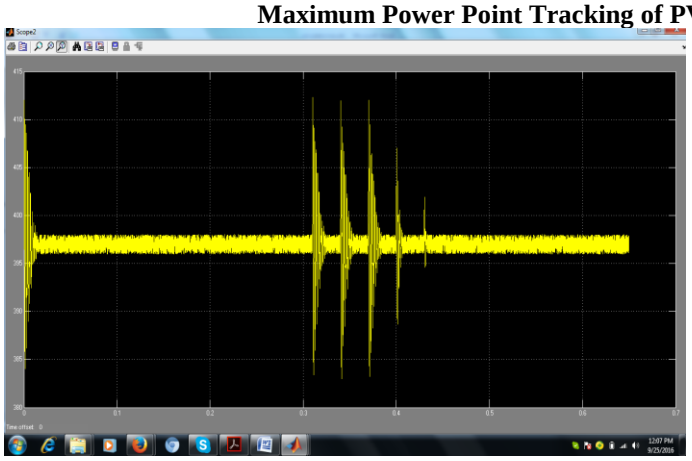

Fig14. DC converter output voltage.

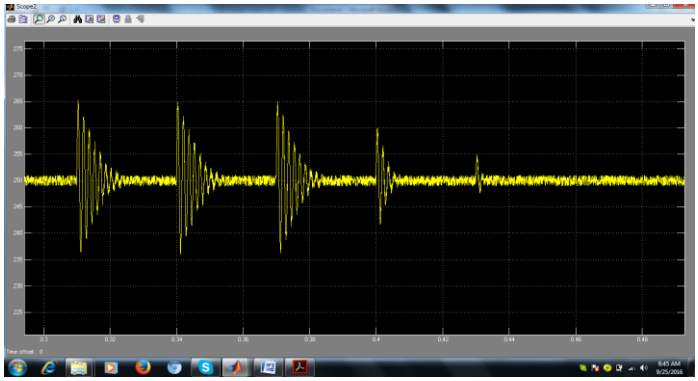

Fig15. DC Converter output voltage with zoomed.

Fig16. Simulation results for input voltage and reference voltage.

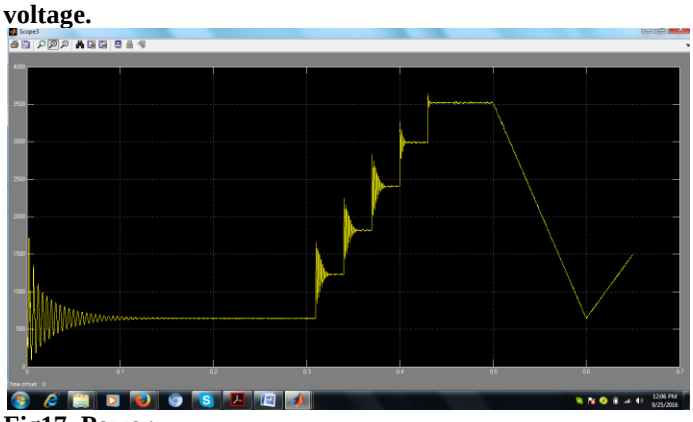

Fig17. Power.

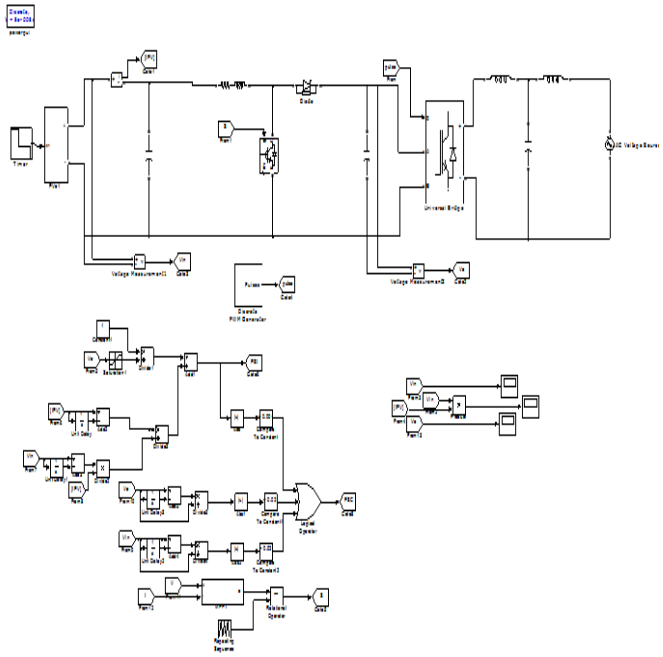

Fig18. Complete Simulink model with conventional method.

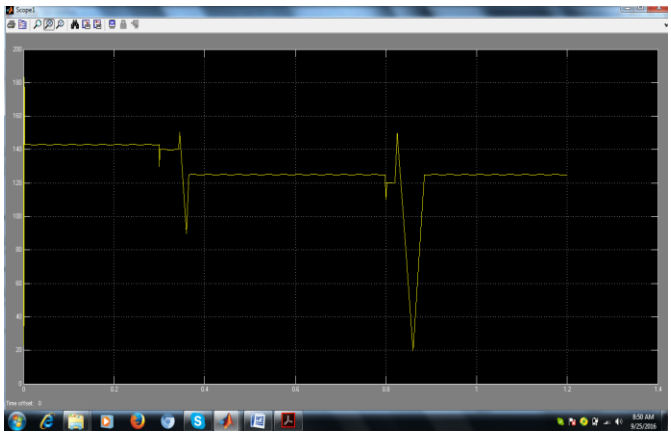

Fig19. Simulation result for input voltage with proposed method.

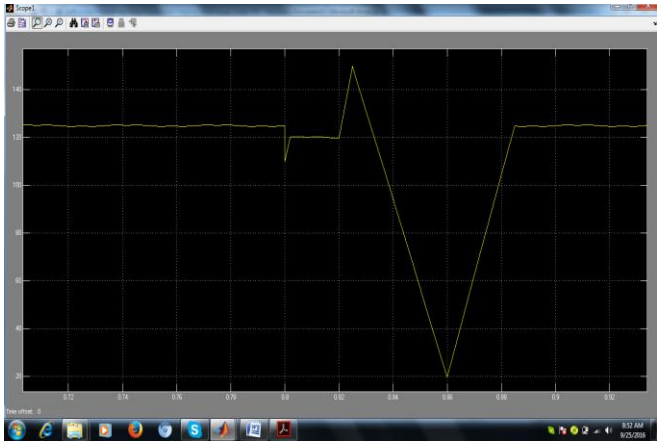

Fig20. Simulation result for input voltage with proposed method zoomed.

Fig21. Simulation result for power with proposed method

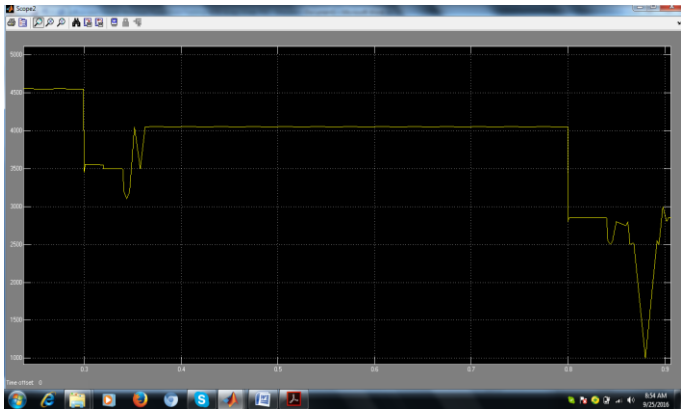

Fig22. Simulation result for input power with proposed method zoomed.

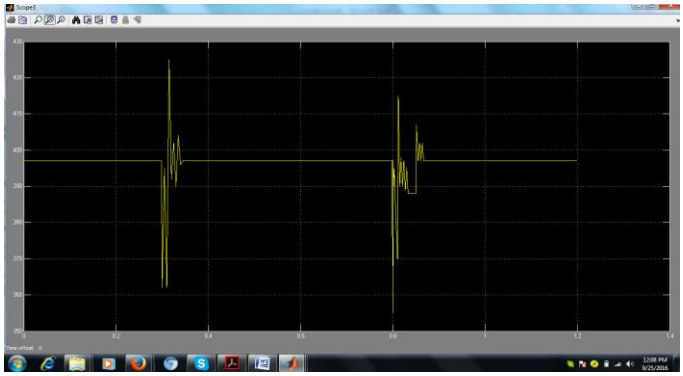

Fig23. Grid voltage with proposed method

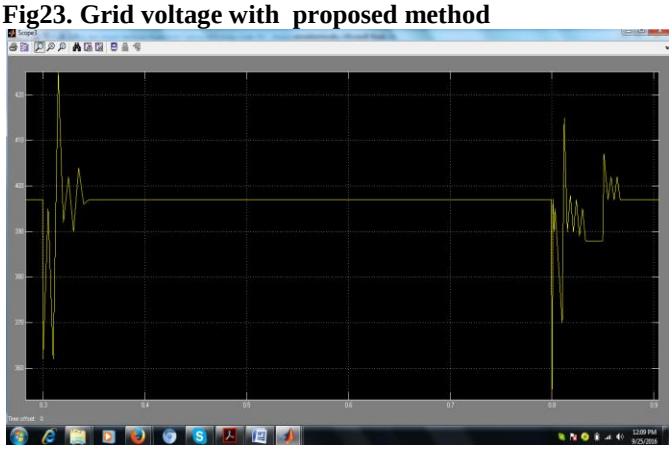

Fig24. Grid Voltage Zoomed.

VII. CONCLUSION

In this project, first a PSC detection algorithm is presented and its performance is studied in different situations. The proposed algorithm determines whether the system operates at uniform irradiance or not. A novel simple and fast algorithm is then presented for MPPT under PSC that operates as direct control method and needs no feedback control of current and voltage. The algorithm is based on ramp change of PV array voltage and simultaneous sampling of its voltage and current continuously. Simulation and experimental results validate the performance of the proposed method in speed and accuracy. The proposed GMPPT method has the following benefits:

- It is simple and can be implemented with a cheap microcontroller like AVR,
- it has a high adjustable speed,
- because of the smooth change of power in comparison with other methods, it has minimum negative impact on the connected power system, and
- its efficiency is guaranteed and is not dependent to the model of modules.

VIII. REFERENCES

[1]Esram and P. L. Chapman, "Comparison of photovoltaic array maximum power point tracking techniques," IEEE Trans. Energy Convers.,vol.22, no.8, pp. 439–449, Jun. 2007.

[2]Y.-J. Wang and P.-C. Hsu, "An investigation on partial shading of PV modules with different connection configurations of PV cells," Energy, vol. 36, pp. 3069–3078, 2011.

[3]D. Kun, B. XinGao, L. HaiHao, and P. Tao, "A Matlab-Simulink-based PV module model and its application under conditions of nonuniform irradiance," IEEE Trans. Energy Convers., vol. 27, no. 4, pp. 864–872, Dec. 2012.

[4]J. Young-Hyok, J. Doo-Yong, K. Jun-Gu, K. Jae-Hyung, L. Tae-Won, and W. Chung-Yuen, "A real maximum power point tracking method for mis-matching compensation in PV array under partially shaded conditions," IEEE Trans. Power Electron., vol. 26, no. 4, pp. 1001–1009, Apr. 2011.

[5]E. Koutroulis and F. Blaabjerg, "A new technique for tracking the global maximum power point of pv arrays operating under partial-shading con-ditions," IEEE J. Photovolt., vol. 2, no. 2, pp. 184–190, Apr. 2012.

[6]N. Tat Luat and L. Kay-Soon, "A global maximum power point track-ing scheme employing direct search algorithm for photovoltaic systems," IEEE Trans. Ind. Electron., vol. 57, no. 10, pp. 3456–3467, Oct. 2010.

[7]S. Syafaruddin, E. Karatepe, and T. Hiyama, "Artificial neural network-polar coordinated fuzzy controller based maximum power point tracking control under partially shaded conditions," IET Renewable Power Gener-ation, vol. 3, pp. 239–253, 2009.

[8]I. Abdalla, J. Corda, and L. Zhang, "Multilevel DC-link inverter and control algorithm to overcome the PV partial shading," IEEE Trans. Power Electron., vol. 28, no. 1, pp. 14–18, Jan. 2013.

[9]P. Sharma and V. Agarwal, "Exact maximum power point tracking of grid-connected partially shaded PV source using current compensation concept," IEEE Trans. Power Electron., vol. 29, no. 9, pp. 4684–4692, Sep. 2014.

[10]C. Woei-Luen and T. Chung-Ting, "Optimal balancing control for tracking theoretical global MPP of series PV modules subject to partial shading," IEEE Trans. Ind. Electron., vol. 62, no. 8, pp. 4837–4848, Aug. 2015.